

Toward Semi-autonomous Stiffness Adaptation of Pneumatic Soft Robots: Modeling and Validation

Majid Roshanfar
Robotics Surgery Lab.
Mechanical Engineering Dept.
Concordia University

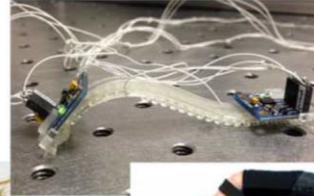
Dr. Javad Dargahi
Robotics Surgery Lab.
Mechanical Engineering Dept.
Concordia University

Dr. Amir Hooshier
Surgical Robotics Centre
Department of Surgery
McGill University

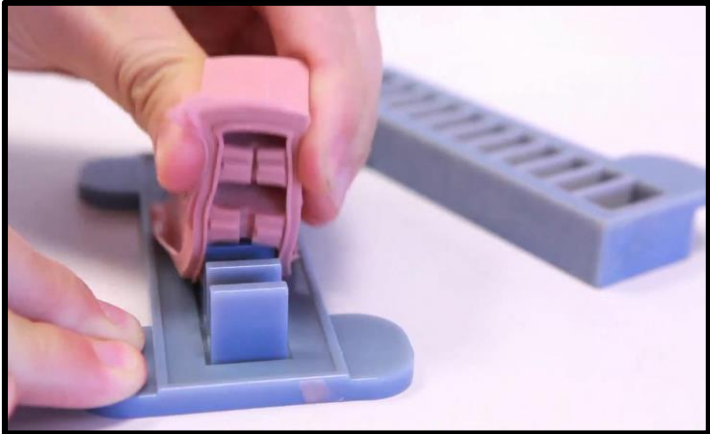
Outline

1. Introduction,
2. Problem Definition,
3. Proposed Solution,
4. Related Studies,
5. Mechanistic Modeling,
6. Validation Study and Results,
7. Conclusion and Future Works.

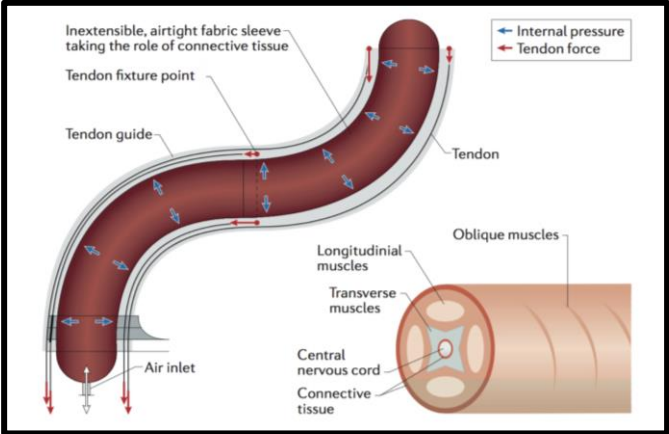
Introduction

iSprawl	Soft gripper	OCTOPUS	Universal gripper	Tuft Softworm	Inflatable robotic arm
					
					
X-RHex	Soft robotic fish	PoseiDrone	Origami robot	Rehabilitation glove	Octobot
Mostly stiff Few selectively compliant elements					Entirely soft

Images from: "Soft robotics: Technologies and systems pushing the boundaries of robot abilities", Cecilia Laschi et al. (2016)



Soft Robotics Toolkit



K. Althoefer et. al. (2018)

Problem Definition

- The constant stiffness of the soft medical robots imposes a cap on their force transmission capacity.

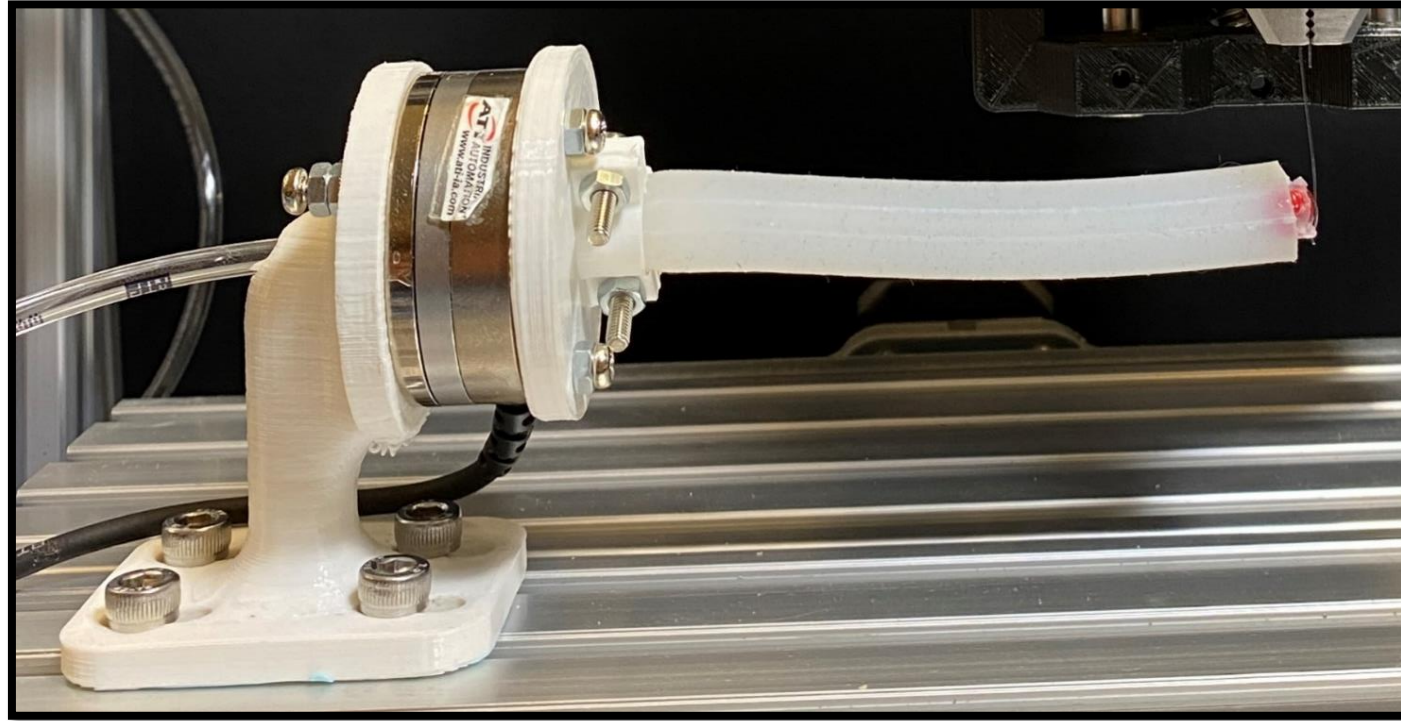


Catheter positioning surgical robot Sensei® X by Hansen Medical, USA – California

Limitation: They possess a pre-determined maneuverability and force transmission range.

Dilemma in the usability of soft surgical robots: Low stiffness is desirable for steerability; However, performing a specific task requires force transmission to the environment.

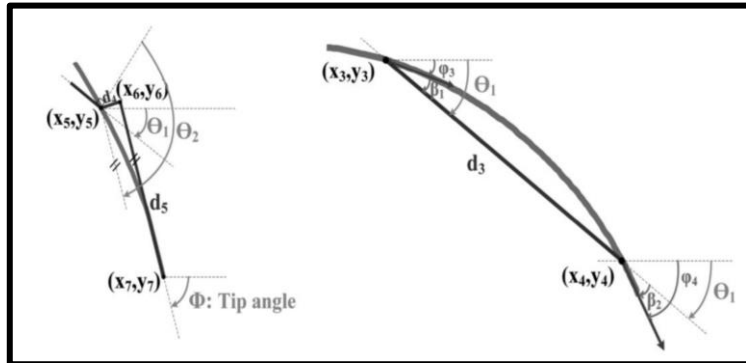
Proposed Solution: Variable Stiffness Soft Robot



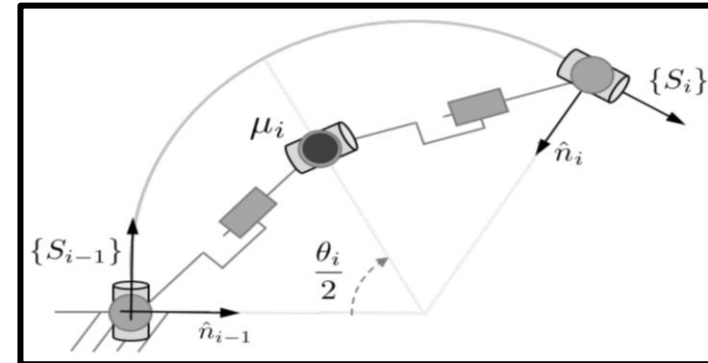
- Stiffness of the soft robot can be decreased during the steering phase for high deformability and increased while performing tasks for high force transmission.

Related Studies

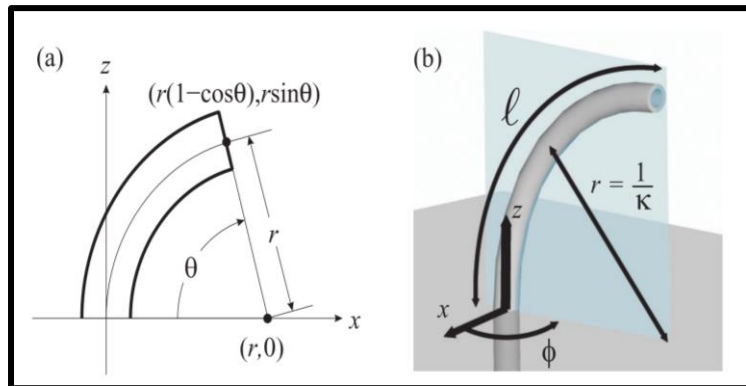
- Soft robots \rightarrow Infinite DoFs \rightarrow Shape approximation methods:



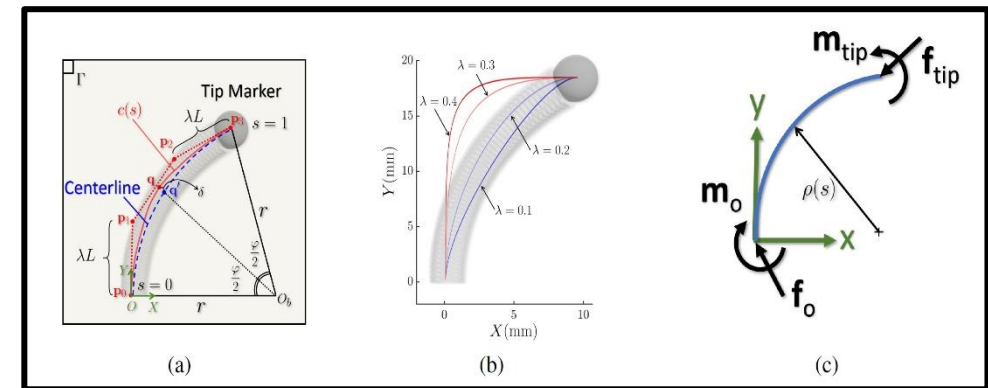
Shape as a curve (M. Khoshnam et al., 2015)



Shape as a set of small rigid segments with soft joints (RK. Katzschmann et al., 2019)



Piecewise constant curvature (RJ Webster III et al., 2010)



Cosserat rod model (Amir Hooshier et al., 2020)

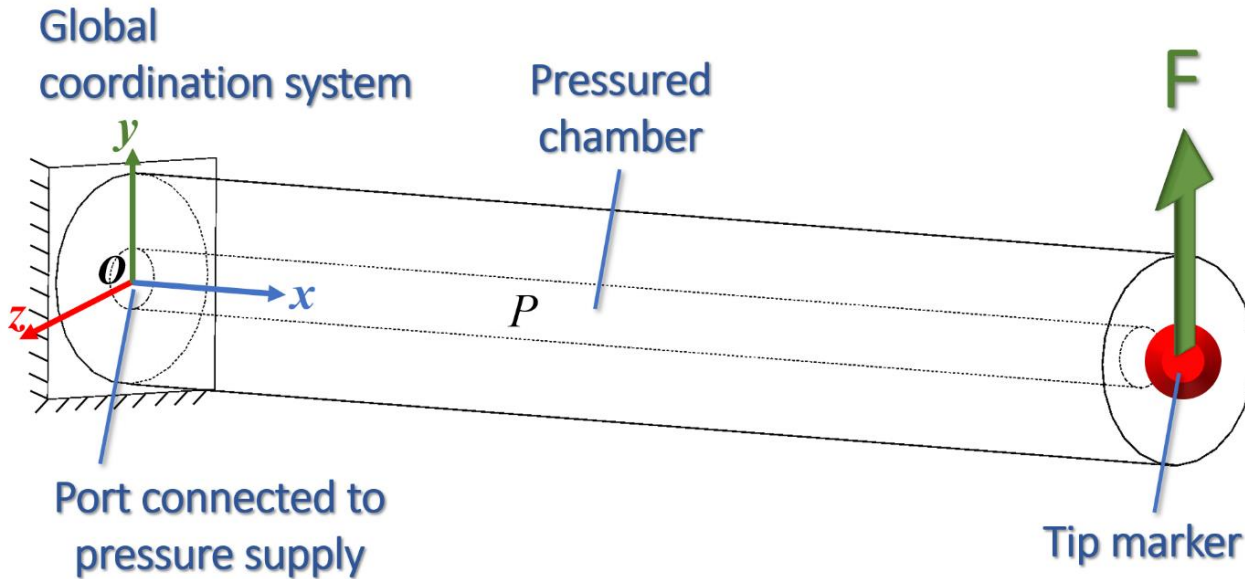
Motivation:

- Propose and validate a mechanistic model to investigate the effects of chamber pressure on the stiffness of the pneumatic-driven soft robots.

Contributions:

1. Modeling the deformation of a single-chamber pneumatic driven soft flexure using Cosserat rod model,
2. Solution of the Cosserat model for a given tip force as an initial value problem (IVP),
3. Validation of the proposed model through experimentation,
4. Demonstrating the feasibility of stiffness modulation by changing the chamber pressure.

Mechanistic Modeling: Kinematics



A : cross-sectional area in its initial shape,

P : internal pressure,

F : external tip force,

s : arc parameter $[0;L]$,

$\mathbf{R}(s)$: locally orthonormal frame,

$\mathbf{p}(s)$: position vector,

$\mathbf{v}(s)$: extension and shear strains along the backbone,

$\mathbf{u}(s)$: bending and torsion strains along the backbone.

$$\mathbf{v}(s) = \mathbf{R}^T(s) \frac{\partial \mathbf{p}(s)}{\partial s}$$

$$\mathbf{u}(s) = \left(\mathbf{R}^T(s) \frac{\partial \mathbf{R}(s)}{\partial s} \right)^\vee$$

Mechanistic Modeling: Conservation of Momentum

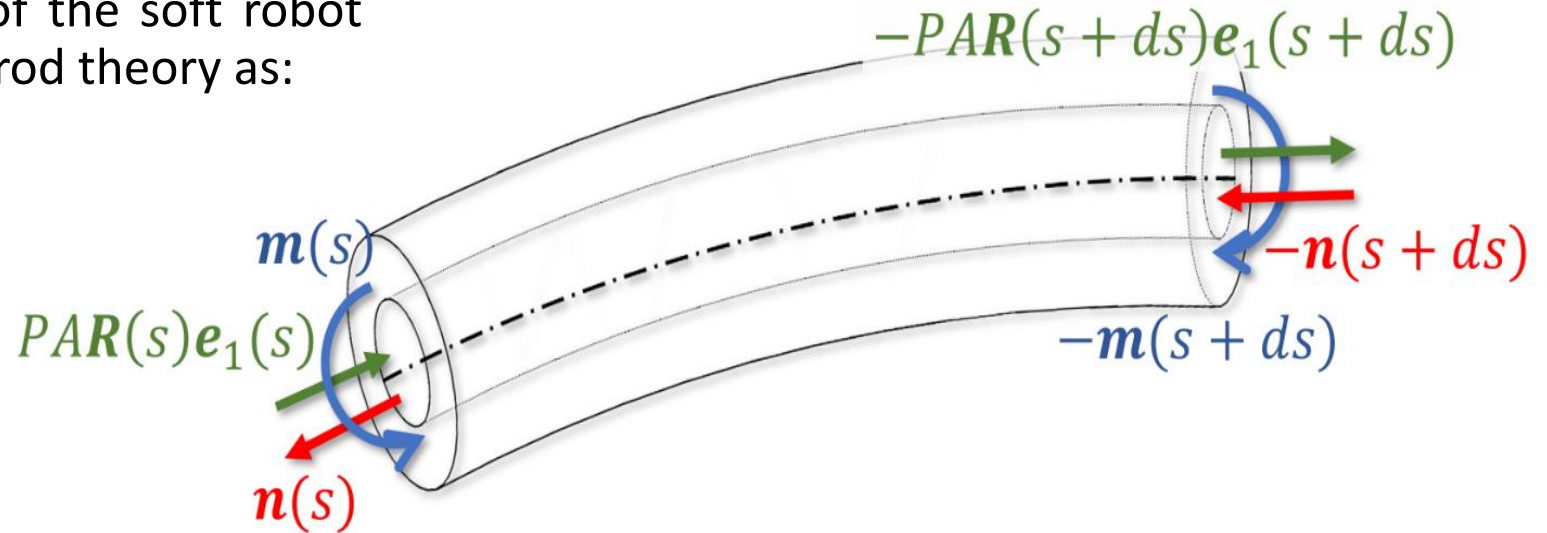
- The quasi-static balance equations of the soft robot were obtained by using the Cosserat rod theory as:

$$\frac{\partial \mathbf{p}(s)}{\partial s} = \mathbf{R}(s)\mathbf{v}(s),$$

$$\frac{\partial \mathbf{R}(s)}{\partial s} = \mathbf{R}(s)(\mathbf{u}(s))^\wedge,$$

$$\frac{\partial \mathbf{n}(s)}{\partial s} = -\rho A \mathbf{g} - P A \mathbf{e}_3(s),$$

$$\frac{\partial \mathbf{m}(s)}{\partial s} = - \left(\frac{\partial \mathbf{p}(s)}{\partial s} \right)^\wedge \mathbf{n}(s),$$



$\mathbf{n}(s)$: internal force vectors in the global coordination system,
 $\mathbf{m}(s)$: internal moment vectors in the global coordination system,
 ρ : material density (constant)
 \mathbf{g} : gravity vector

Mechanistic Modeling: Constitutive Equations

- Two-term Mooney-Rivlin (2MR) constitutive model for the material behavior of the soft robot for uniaxial elongation:

$$T_{11} = 2\left(c_{01} + \frac{c_{10}}{\lambda}\right)(\lambda^2 - \lambda^{-1})$$

T_{11} : longitudinal nominal stress,

λ : longitudinal stretch,

c_{01} and c_{10} : material constants.

- Based on the Cosserat rod model, the linear elastic constitutive equations are:

$$\mathbf{n}(s) = \mathbf{R}(s)\mathbf{K}_{se}\left(\mathbf{v}(s) - \mathbf{v}^*(s)\right)$$

$$\mathbf{m}(s) = \mathbf{R}(s)\mathbf{K}_{bt}\left(\mathbf{u}(s) - \mathbf{u}^*(s)\right)$$

- By substituting the derived shear and Hooke's Moduli, the tangent stiffness matrices is:

$$\mathbf{K}_{se} = \text{diag}\left(E_oA \quad G_oA \quad G_oA\right)$$

$$\mathbf{K}_{bt} = \text{diag}\left(2G_oI \quad E_oI \quad E_oI\right)$$

Mechanistic Modeling: Solution

- Runge-Kutta (RK4) method with a step-size of $\delta_s = \frac{L}{100}$
- Dirichlet and Neumann boundary conditions at $s = 0$ that were formulated as:

$$\mathbf{p}(s)|_{s=0} = (0 \quad 0 \quad 0)^T,$$

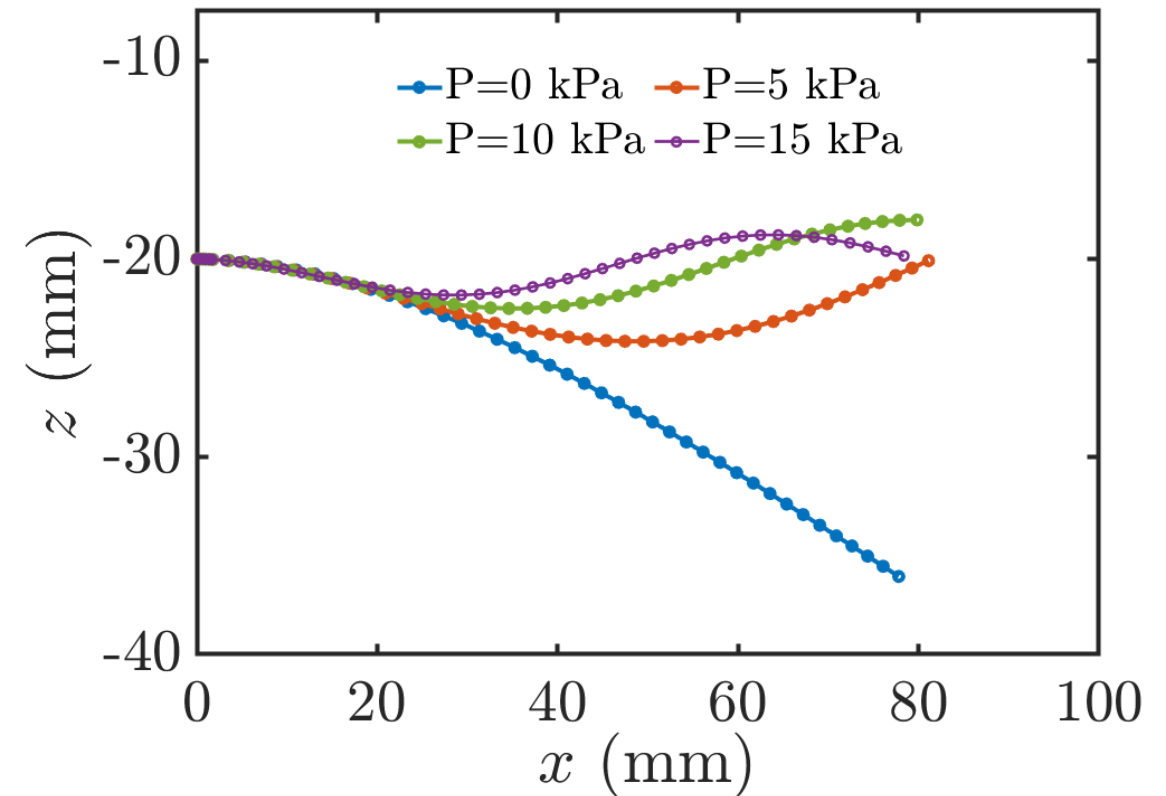
$$\mathbf{u}(s)|_{s=0} = (1 \quad 0 \quad 0)^T,$$

$$\mathbf{R}(s)|_{s=0} = \mathbf{I}_{3 \times 3},$$

$$\mathbf{v}(s)|_{s=0} = \mathbf{0}.$$

Model parameters of the prototyped soft robot.

Parameter	Length L (mm)	Outer Dia. D_o (mm)	Inner Dia. D_i (mm)	2MR Constants		Density ρ ($\frac{g}{cc}$)
				c_{01} (kPa)	c_{10} (kPa)	
	85	12	3.5	277	-209	1.04

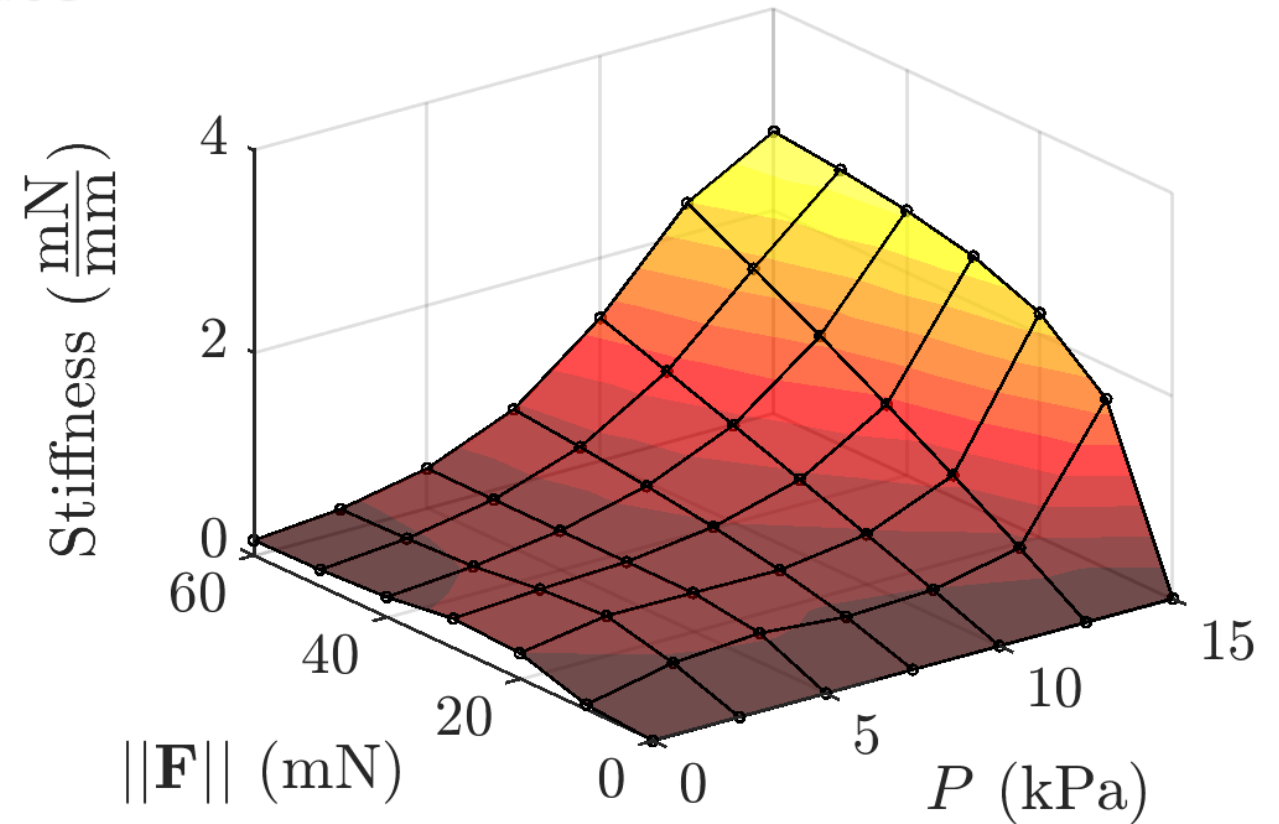


Deformation of the soft robot under its weight and a tip force of 30 mN in +z-direction with various chamber pressures.

Mechanistic Modeling: Stiffness Surface

➤ Stiffness:

$$k = \frac{\partial \|\mathbf{F}\|}{\partial \|\mathbf{p}(s = L)\|} = k(F, P)$$



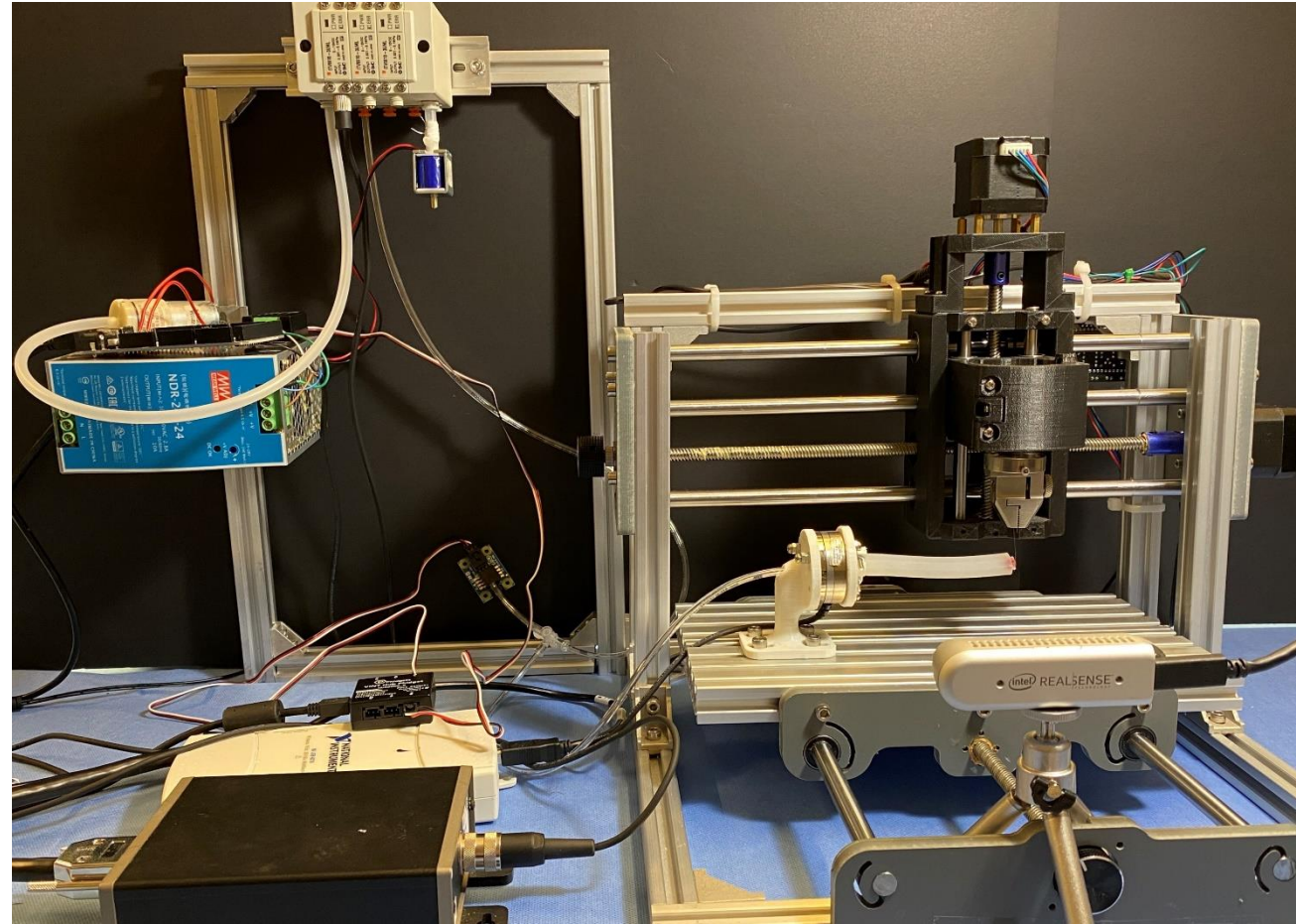
Variation of the soft robot's stiffness with internal pressure and tip force.

Validation Study: Setup

- Pressure regulator: ITV0010-3UML, SMC, Tokyo, Japan
- Desktop CNC
- RGB-D camera: D435i, Intel Corp., CA, USA
- Force Sensor: ATI Industrial Automation, F/T Sensor, Mini40

Validation Study: Protocol

- Pressure range: 0 – 20 kPa
- Tip displacement: 0 – 15 mm
- Force range: 0 – 89 mN

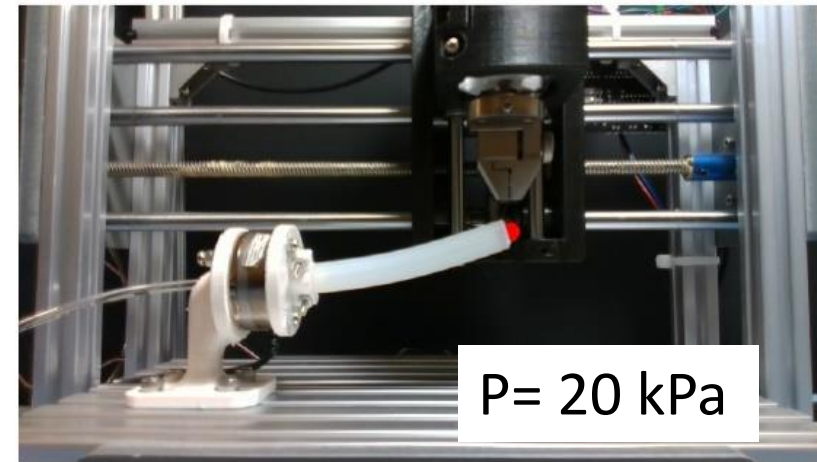
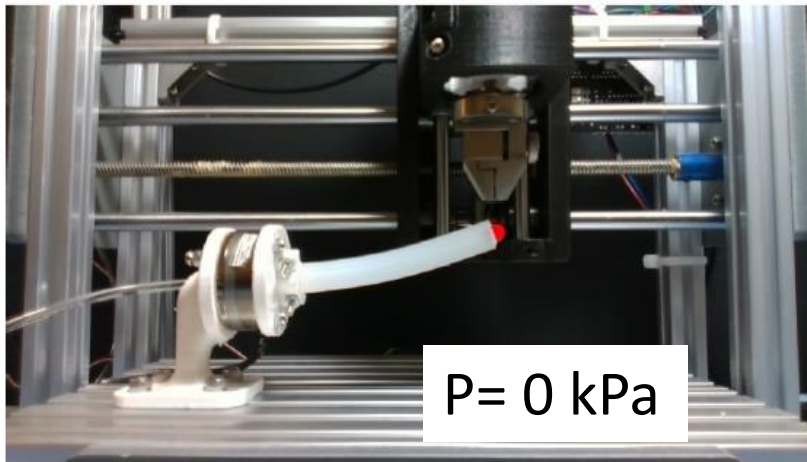


Validation Study: Results

- Stiffness of the soft robot increased from $3.4 \frac{mN}{mm}$ (P=0 kPa) to $5.9 \frac{mN}{mm}$ (P=20 kPa) indicating a 74% pressure-stiffening effect.

Comparison of the model results with experiments.

Pressure (kPa)	Tip Force (mN)	Tip Displacement		Displacement Error		Stiffness (mN/mm)
		Model (mm)	Reference (mm)	Absolute (mm)	Relative (%)	
0	51	14.4	15	0.6	3.4%	3.4
4	64	14.3	15	0.7	4.7%	4.3
12	73	13.9	15	1.1	7.3%	4.9
20	89	13.7	15	1.3	8.7%	5.9

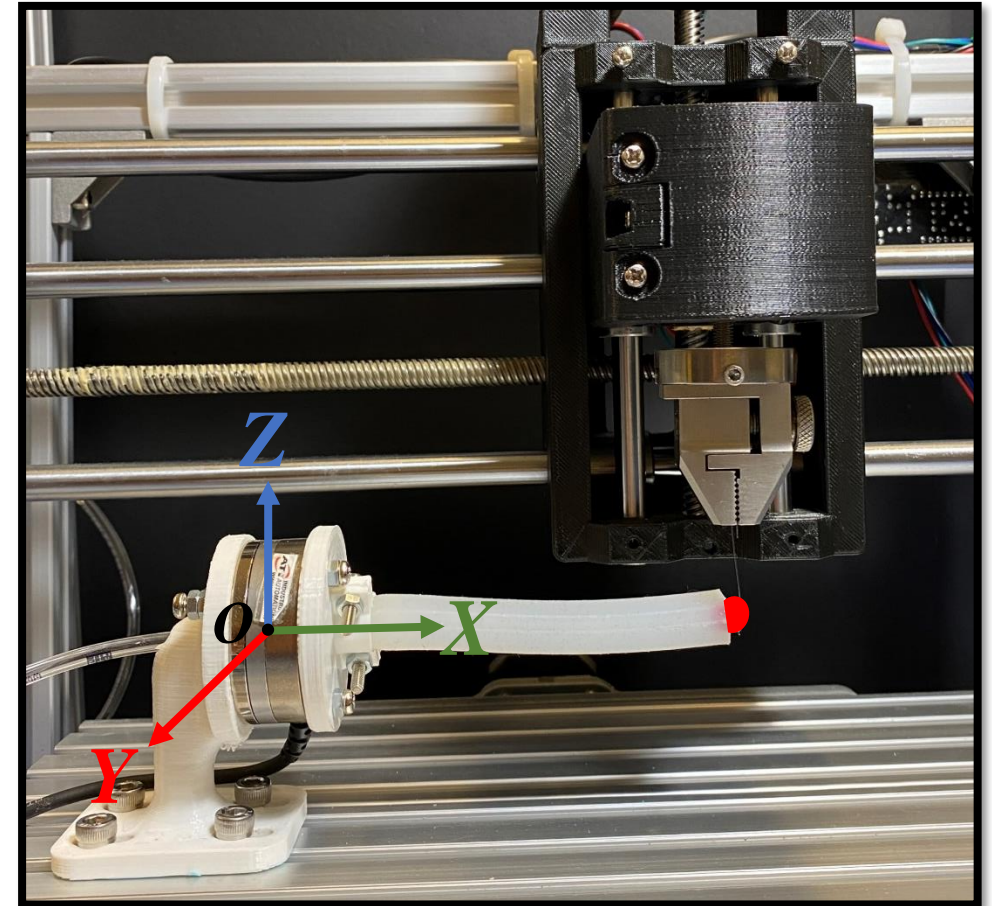


Conclusion:

- IVP with homogeneous Neumann and Dirichlet boundary conditions,
- Comparison of the theoretical findings with experimental results for tip displacement and stiffness showed similar trends with a maximum error of 8.7%,
- The findings confirmed the feasibility of stiffness adaptation through chamber pressure regulation.

Future works:

- Exploiting the pressure-stiffening phenomenon for stiffness adaptation of soft surgical robots during interventional procedures,
- Effects of presence of multiple chambers for directional stiffening,
- Feasibility of position-stiffness hybrid control through tendon-pneumatic actuation.



Thank You